

# REDUCTION OF MAGNETIC AND TRANSVERSE ELECTRIC SCATTERING AMPLITUDES IN $^{207}\text{Pb}$ BY CORE POLARIZATION

I. HAMAMOTO<sup>1,2</sup>

*Center for Theoretical Physics, Laboratory for Nuclear Science and Department of Physics,  
M.I.T., Cambridge, MA. 02139, USA*

J. LICHTENSTADT<sup>1,3</sup>

*Bates Linear Accelerator Center, Laboratory for Nuclear Science and Department of Physics,  
M.I.T., Cambridge MA. 02139, USA*

and

G.F. BERTSCH<sup>4</sup>

*Department of Physics and Cyclotron Laboratory Michigan State University, East Lansing MI 38824, USA*

Received 17 August 1980

It is shown that core-polarization causes a considerable reduction of the nuclear magnetization current at high momentum transfer irrespective of multipolarity. The reduction is consistent with the observed reduction of both magnetic and transverse electric form factors in the  $^{207}\text{Pb}$  and  $^{208}\text{Pb}$  nuclei. No corresponding systematic reduction is expected in the nuclear convection current.

In recent high resolution electron scattering experiments on  $^{207}\text{Pb}$  [1,2] the low lying neutron hole excitations have been studied. It has been observed that there is a systematic reduction of the transverse scattering amplitude to about 55% of the single particle value, independent of the transition multipolarity and the momentum transfer investigated. Various mechanisms were suggested to explain this reduction. In this letter we present a calculation of the core polarization effect on the nuclear magnetization currents which accounts for a substantial part of this reduction in both magnetic and electric transitions. We use the same model [3] by which a similar reduction was obtained in the high spin transitions ( $J^\pi = 12^-, 14^-$ ) in  $^{208}\text{Pb}$  [4]. While in the latter only the first maxima of the magnetic form factors have been measured those of

the low multipolarity transitions discussed here exhibit several peaks in the probed momentum transfer range and provide an opportunity to study the core polarization effect via electric and magnetic transitions with different multiplicities and different forms of wave functions involved.

The states discussed here are at 0.571 MeV ( $3p_{1/2} \rightarrow 2f_{5/2}$ ), 0.899 MeV ( $3p_{1/2} \rightarrow 3p_{3/2}$ ), 1.634 MeV ( $3p_{1/2} \rightarrow 1i_{13/2}$ ), and at 2.340 MeV ( $3p_{1/2} \rightarrow 2f_{7/2}$ ). In each of these the neutron-hole configuration (mentioned) is supposed to be the overwhelmingly predominant component in both the initial and final states (denoted by  $p_0$  and  $p_1$  respectively). Thus we estimate the core-polarization by perturbation. We obtain the following inhomogeneous equation [3,5,6] for the perturbed particle wave-function  $X_{ph}(r)$ :

$$\left[ \frac{\hbar^2}{2m} \left( -\frac{d^2}{dr^2} + \frac{l_p(l_p+1)}{r^2} \right) + V(r) - (\epsilon_{p_1} - \epsilon_{p_0} + \epsilon_h) \right] \\ \times rX_{ph}(r) = -rR_h(r)R_{p_0}(r)R_{p_1}(r) \sqrt{\frac{2\lambda+1}{2j_{p_0}+1}} (-1)^{j_{p_0}+j_{p_1}+\lambda}$$

<sup>1</sup> Supported in part by U.S. D.O.E. contract No. DE-AC0276 ER03069.

<sup>2</sup> Address after Sept. 1980: Nordita, Blegdamsvej 17, Copenhagen, Denmark.

<sup>3</sup> Address after Sept. 1980: Tel-Aviv University, Tel-Aviv, Israel.

<sup>4</sup> Supported in part by the National Science Foundation.

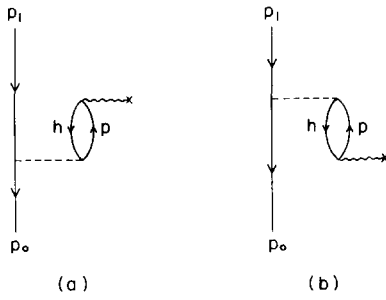


Fig. 1. Core-polarization diagrams included in the present calculation.

$$\langle (Y_{l_p \frac{1}{2}})^{j_p} (Y_{l_h \frac{1}{2}})^{j_h} | v \delta(\Omega_1 - \Omega_2) | (Y_{l_{p_1} \frac{1}{2}})^{j_{p_1}} (Y_{l_{p_0 \frac{1}{2}} \frac{1}{2}})^{j_{p_0}} \rangle_{(1)}$$

of a 1p-2h configuration (denoted by  $p$ ,  $p_1$ , and  $h$ ), which has the total angular momentum  $j_{p_0}$  (fig. 1a). The effective residual interaction was taken to be a  $\delta$ -function, and the eigenvalues of the single-particle Hamiltonian of the orbits  $p_0$ ,  $p_1$  and  $h$  are denoted by  $\epsilon_{p_0}$ ,  $\epsilon_{p_1}$  and  $\epsilon_h$  respectively.  $R(r)$  is the normalized radial wave-function and the single-particle potential  $V(r)$  has the Woods-Saxon form. Numerically we projected out from  $X$  the components below the Fermi sea, though the observables are unaffected by the projection [6]. Then the perturbed particle wave-function  $X_{ph}(r)$  has a normalization given by the probability of the amplitudes in the complete wave-function. Exchanging the role of  $p_0$  with that of  $p_1$ , we obtain the equation for the particle amplitude,  $Y_{ph}(r)$  of a 1p-2h configuration (denoted by  $p$ ,  $p_0$ , and  $h$ ) which has the total angular momentum  $j_{p_1}$  (fig. 1b).

We perform the complete summation over the particle-hole configurations (ph) in fig. 1, by integrating the inhomogeneous differential equation (1) (and the corresponding equation for  $Y_{ph}(r)$ ) for all possible particle-angular momentum  $j_p$  associated with all the occupied orbits  $h$ , and by summing up all the contributions. This way of calculating the core-polarization is free from the inaccuracy due to space truncation inherent in the usual shell-model calculations. Furthermore, the calculated particle wave-functions have the correct asymptotic behaviour at large  $r$ .

As an effective interaction we use a  $\delta$ -interaction with the coefficients  $v = v_{\sigma\sigma} \sigma \cdot \sigma + v_{\sigma\tau} \sigma \cdot \sigma \tau \cdot \tau$  in which the strength was taken to be  $v_{\sigma\sigma} + v_{\sigma\tau} = 170 \text{ MeV fm}^3$ . This is the same effective interaction used in ref. [3]

to calculate the core-polarization effect on the high spin transitions in  $^{208}\text{Pb}$ . The interaction strength was discussed in the same article [3].

The electron scattering cross section is given in the Born approximation by:

$$\frac{d\sigma}{d\Omega} = \frac{d\sigma_M}{d\Omega} \eta \left[ \sum_{J=0}^{\infty} F_{cJ}^2 + \left( \frac{1}{2} + \tan^2 \frac{\theta}{2} \right) \sum_{J=1}^{\infty} (F_{EJ}^2 + F_{MJ}^2) \right];$$

$$\frac{d\sigma_M}{d\Omega} = \frac{Z^2 \alpha^2}{q^2 \tan^2 \theta/2}, \quad (2)$$

and the recoil factor:  $\eta = [1 + (2E_e/M_t) \sin^2 \theta/2]^{-1}$ .

The  $J = \frac{1}{2}$  ground state of  $^{207}\text{Pb}$  limits the sum over the multiplicities in (2) to one electric and one magnetic transitions in each excitation. The three form factors  $F_{cJ}$ ,  $F_{EJ}$  and  $F_{MJ}$  are related to the nuclear charge, convection-current and magnetization-current densities [7]. The expressions for  $F_{MJ}$  and  $\rho_{JJ}$  were given in ref. [3]. The transverse electric form-factor,  $F_{EJ}$ , is related to the transition current densities  $\tilde{\rho}_{JJ-1}$ , and  $\tilde{\rho}_{JJ+1}$ , in the Born approximation by:

$$F_{EJ}(q) = \frac{\sqrt{4\pi}}{Z} \sqrt{\frac{2J_f+1}{2J_i+1}}$$

$$\times \int r^2 dr \left[ \sqrt{\frac{J+1}{2J+1}} \tilde{\rho}_{JJ-1}(r) j_{J-1}(q_r) \right.$$

$$\left. + \sqrt{\frac{J}{2J+1}} \tilde{\rho}_{JJ+1}(r) j_{J+1}(q_r) \right]. \quad (3)$$

The transverse electric transition current density (before including the corrections due to the nucleon finite size) can be written as:

$$\rho_{JJ\pm 1}(r) = \rho_{JJ\pm 1}^{(l)}(r) + \rho_{JJ\pm 1}^{(s)}(r), \quad (4)$$

with the convection current:

$$\rho_{JJ\pm 1}^{(l)}(r) = g_l^j \frac{\hbar}{mc} \frac{1}{\sqrt{2J_f+1}} (-1)^{1/2 \pm 1/2}$$

$$\times \left[ f_{J,J\pm 1,1}^{(+)(p_1,p_0)} R_{p_1}(r) \left( \frac{d}{dr} - \frac{l_{p_0}}{r} \right) R_{p_0}(r) \right.$$

$$+ \sum_{ph} f_{J,J\pm 1,1}^{(+)(ph)} (X_{ph}(r) + Y_{ph}(r)) \left( \frac{d}{dr} - \frac{l_h}{r} \right) R_h(r)$$

$$+ f_{J,J\pm 1,1}^{(-)(p_1,p_0)} R_{p_1}(r) \left( \frac{d}{dr} + \frac{l_{p_0}+1}{r} \right) R_{p_0}(r) \quad (5)$$

$$\left. + \sum_{ph} f_{J,J\pm 1,1}^{(-)(ph)} (X_{ph}(r) + Y_{ph}(r)) \left( \frac{d}{dr} + \frac{l_h+1}{r} \right) R_h(r) \right]$$

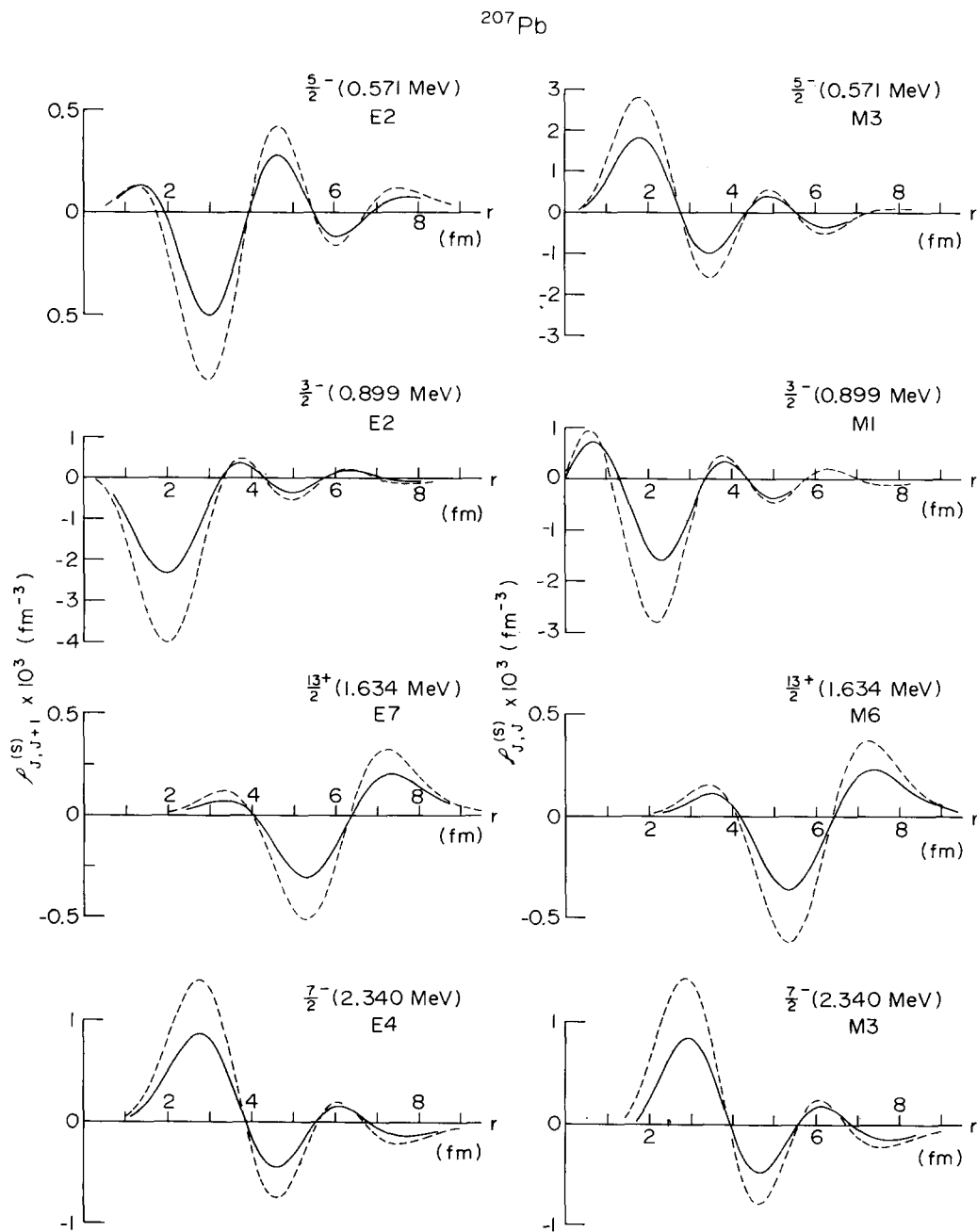


Fig. 2. Transition current densities in  $^{207}\text{Pb}$  calculated by using the pure single-particle and the perturbed wave functions (dashed and solid lines respectively). The pure single-particle wave functions were calculated using a Woods Saxon potential with the same parameters as in ref. [3].

and the magnetization current:

$$\begin{aligned} \rho_{JJ+1}^{(s)}(r) = & \mu^i \frac{\hbar}{mc} \frac{1}{\sqrt{2J_f+1}} \sqrt{\frac{J+(1\mp 1)/2}{2J+1}} \\ & \times \left[ \langle j_{p1} \| (Y_J s)_{(J1)J} \| j_{p0} \rangle \left( \frac{J+(1\mp 1)/2}{r} \mp \frac{d}{dr} \right) \right. \\ & \times R_{p1}(r) R_{p0}(r) + \sum_{ph} \langle j_p \| (Y_J s)_{(J1)J} \| j_h \rangle \\ & \times \left( \frac{J+(1\mp 1)/2}{r} \mp \frac{d}{dr} \right) (X_{ph}(r) + Y_{ph}(r)) R_h(r) \left. \right]. \quad (6) \end{aligned}$$

where

$$\begin{aligned} f_{JL1}^{(\pm)(ph)} \equiv & (-1)^{\mp \frac{1}{2} + l_p - j_h + L} \\ & \times \sqrt{\frac{(2j_h+1)(2j_p+1)(2L+1)(2J+1)}{4\pi}} W(l_p j_p l_h j_h; \frac{1}{2} J) \\ & \times \sqrt{(l_h + (1\pm 1)/2)(2l_h + 2(1\pm 1) - 1)} \\ & \times (l_h \pm 1, L, l_p; 0 0 0) W(l_h 1 l_p L; l_h \pm 1, J), \\ \mu^\pi = & 2.79, \quad \mu^\nu = -1.91, \quad g_l^\pi = 1, \quad g_l^\nu = 0. \quad (7) \end{aligned}$$

The convection and magnetization current densities were then folded with the respective nucleon charge and magnetization densities.

Even though the major contribution to the electric single neutron transitions are due to its magnetic moment, it has been shown that these transitions have a Coulomb form factor due to induced charge [9]. This Coulomb form-factor has a non-negligible contribution even at  $160^\circ$  (at which experimental data exists). It can be accounted for [1,2] by taking the transition charge density of the corresponding collective excitations in  $^{208}\text{Pb}$ , scaled down to fit the forward scattering data [9]. The electron scattering cross sections shown below were calculated in the distorted wave Born approximation (DWBA), using the densities discussed above. For the electric transition form-factors which in DWBA cannot be separated into the longitudinal and the transverse parts, the "experimental" charge density was taken [1] in addition to the calculated (and folded) current densities, using the DWBA code HEITRA [10]<sup>†</sup>. The magnetic calculations were done using the code HEIMAG [10].

<sup>†</sup> The DWBA code HEITRA accepts the transition charge density and only the part of the current density,  $\rho_{JJ+1}$ , calculating the other part  $\rho_{JJ-1}$  by the continuity equation. The current  $\rho_{JJ-1}$  calculated by the program was compared to the one calculated theoretically, and they did not differ by more than 6% and only in the peaks at small radii.

The calculated current densities using the perturbed and the pure single-particle wave-functions are shown in fig. 2. A considerable reduction of the current is predicted for the various multipolarities. A comparison between the calculated ( $e, e'$ ) cross sections (using these densities), and the experimental data is shown in fig. 3a with rather good agreement between the two.

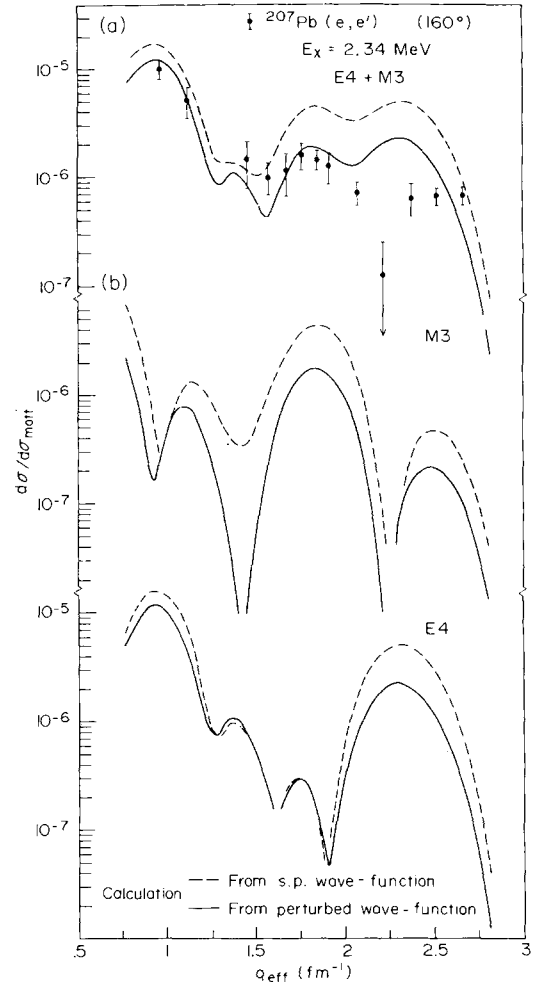


Fig. 3. (a) Comparison between experimental data and the calculated ( $e, e'$ ) form-factor for the transition to the  $7/2^-$  state at 2.34 MeV. The densities from fig. 2 were used, and the calculation was done in DWBA.  $q_{\text{eff}} = q(1 + 4Z\alpha/3EA^{1/3})$ . The dashed lines are calculations using the densities obtained from the unperturbed wave-functions while the solid lines are those using the perturbed ones. (b) Individual contributions of the magnetic (M3) and the electric (E4) (longitudinal and transverse) transitions to the total ( $e, e'$ ) cross section shown in part a.

Similar comparisons were obtained for the other transitions for which preliminary data exist [1]. The particular example shown in fig. 3 indicates that the peak in the E4 transition around  $q = 2.3 \text{ fm}^{-1}$  is not sufficiently reduced due to the present mechanism, compared with the experimental data. For reference we also show the cross sections calculated from densities using the unperturbed single-particle wave-functions. In fig. 3b we show the individual contributions of the magnetic and the electric (longitudinal and transverse) transitions to the cross section. The major reduction in the current which is predicted at small radii, corresponds to the reduction in the peak of the form-factor in the high momentum transfer region. It should be noted that the reduction at low momentum transfer is not easily seen due to the contributions from the longitudinal form-factor in this region.

We stress the comparison of peak heights at the high momentum transfer region since we have used here a  $\delta$ -interaction as an effective interaction with a given strength, which might not be valid for the entire momentum transfer region. The numerical results show that the sum of the probabilities in the admixed configurations is always less than one percent. It justifies the use of a perturbation calculation in the present case.

Since a lot of configurations contribute to the polarization at high momentum transfer, one may expect that the results in finite nuclei would be pretty much independent of the multipolarity, and would be approximately estimated by the Fermi-gas model. We have shown in ref. [3] that in an infinite Fermi-gas a static polarization of  $-0.28$  is obtained at maximum momentum transfer across the Fermi-surface ( $q = 2k_F$ ), by using our effective interaction. The cross section is correspondingly reduced then by a factor of  $(1-0.28)^2 = 0.52$ . This factor is in good agreement with the observations in the  $^{208}\text{Pb}$  region and our numerical calculations. In contrast a polarization at low momentum transfer depends on a rather limited number of configurations and as such would be sensitive to the shell struc-

ture and consequently to the multipolarity.

It should be mentioned that the calculated reduction of both MJ and EJ form-factors in the present case stems essentially from the renormalization of the magnetization currents  $\rho_{JL}^{(s)}$ . The calculated convection current density shows generally only a small reduction (or sometimes even a slight enhancement) due to the core-polarization. We expect then that the appreciable reduction of the transverse form-factors from the pure shell model values will not be observed between certain proton configurations of which a predominant contribution to the transverse form factor stems from the convection current.

We would like to thank Drs. J. Heisenberg and C.N. Papanicolas for the helpful discussions. One of the authors (I.H.) would like to thank the Center for Theoretical Physics at M.I.T. for its warm hospitality.

### References

- [1] C.N. Papanicolas, Ph.D. Thesis M.I.T. (1979).
- [2] C.N. Papanicolas, J. Lichtenstadt, C.P. Sargent, J. Heisenberg and J.S. McCarthy, Phys. Rev. Lett., to be published.
- [3] I. Hamamoto, J. Lichtenstadt and G.F. Bertsch, Phys. Lett. B, to be published.
- [4] J. Lichtenstadt, J. Heisenberg, C.N. Papanicolas, C.P. Sargent and J.S. McCarthy, Phys. Rev. 20C (1980) 497.
- [5] B. Buck and A.D. Hill, Nucl. Phys. A95 (1967) 271.
- [6] I. Hamamoto, Phys. Lett. 66B (1977) 66B, and Proc. of Int. School of Phys. "Enrico Fermi", LXIX (1976) p. 258.
- [6] S. Shlomo and G.F. Bertsch, Nucl. Phys. A243 (1975) 507.
- [7] e.g. H.C. Lee, AECL 4839 Chalk-River, Ontario 1975 (unpublished).
- [8] R. Hofstadter et al., Rev. Mod. Phys. 30 (1958) 482; W. Bertozzi et al., Phys. Lett. 41B (1972) 408.
- [9] C.N. Papanicolas, J. Heisenberg, J. Lichtenstadt, A.N. Courtemanche and J.S. McCarthy, Phys. Rev. Lett. 41 (1978) 537.
- [10] J. Heisenberg, Codes HEITRA and HEIMAG, unpublished.